J|A|C|S
COMMUNICATIONS

Published on Web 03/23/2006

Experimental Investigation of Particle-Assisted Wetting

Ailin Ding and Werner A. Goedel*

Chemnitz University of Technology, Physical Chemistry, Strasse der Nationen 62, Chemnitz D-09111, Germany

Received December 6, 2005; E-mail: werner.goedel@chemie.tu-chemnitz.de

The wetting of *solids* is often considered in the literature. The wetting of a *liquid* by a second liquid, on the other hand, has received comparatively less attention. However, the wetting of a liquid by a second liquid is extremely attractive. For example, one might prepare a wetting layer of a polymerizable oil on a water surface, solidify it, transfer it to a solid support, and thus obtain a thin membrane. Unfortunately, there is hardly any liquid that wets a water surface.

Wetting is, in general, determined by an interplay of short-range and long-range forces. Due to the comparatively low refractive index of water, the latter usually are unfavorable. Thus, amphiphiles which influence only short-range forces are inefficient in promoting the wetting of a water surface by an oil. We recently discovered that particles can assist the wetting of a water surface by an oil.[1−3] This principle was utilized for the preparation of freely suspended membranes, especially for membranes of controlled porosity.[4−7] On the other hand, we developed a simple theory describing the principle behind particle-assisted wetting.[8] In general, placing a particle into a liquid/liquid or liquid/air interface gives rise to a gain in energy, which is largest if the contact angle of that interface with the particle is close to 90°.[9,10] If mixtures of an oil and particles are applied to a water surface, the oil might either form lenses completely separated from the particles, or form lenses completely engulfing the particles, or form wetting layers in which the particles penetrate through at least one of the interfaces of that layer. Depending on the interfacial tensions of the air/oil, air/water, oil/water interfaces, and the contact angles of these interfaces with the particles, one can calculate which of the above-mentioned scenarios is energetically most favorable and draw phase diagrams of particle-assisted wetting.[8] Previously we investigated particle-assisted wetting qualitatively using a photopolymerizable oil (trimethylolpropane trimethacrylate, TMPTMA) and a series of irregular-shaped silica particles of various hydrophilicity, but unknown contact angles with the liquid interfaces.[11] At that time, no direct comparison to the theory was possible. Here, we use a series of differently coated spherical silica particles and compare the experimental results directly with the corresponding theoretical phase diagram.

On the basis of the tensions of the interfaces (see caption of Figure 1), one can calculate an equilibrium spreading coefficient of the oil TMPTMA of $S_e = \gamma_{aw} - \gamma_{ao} - \gamma_{wo} = -0.11$ mN/m. The negative value of S_e is in accordance with the fact that TMPTMA alone forms lenses on a water surface. The phase diagram of particle-assisted wetting specific for the oil TMPTMA and dense two-dimensional packing of the particles is shown in Figure 1. The curved lines in Figure 1 indicate coexistence between two scenarios; within a regime enclosed by these lines, the scenario indicated by the corresponding sketch is expected to be energetically most favorable.

Spherical silica particles were prepared by Stöber synthesis[12−14] and then modified by four different silane coupling agents: (a) 3-aminopropyltriethoxysilane, (b) propyltriethoxysilane, (c) 3,3,3-trifluoropropyltrimethoxysilane, and (d) 1*H*,1*H*,2*H*,2*H*-perfluorooctyltriethoxysilane. The contact angles of these particles at the air/water and oil/water interfaces were estimated by measuring the contact angle of oil droplets (in water and in air) on glass slides whose surfaces were treated with the same silane coupling agents. These contact angles determine the position of the four types of particles in the phase diagram (Figure 1).

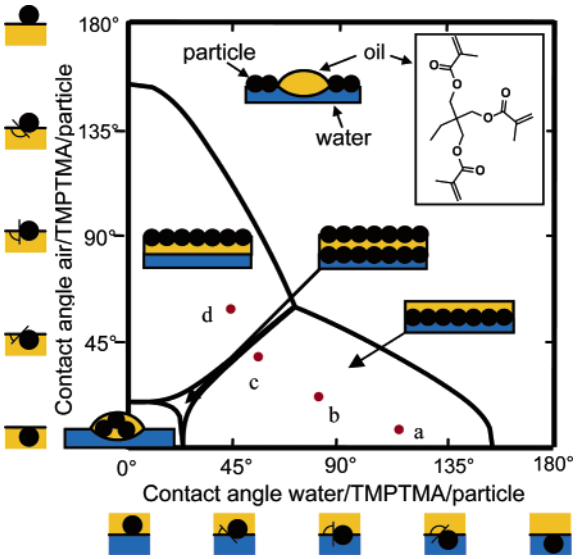

Figure 1. Phase diagram of particle-assisted wetting for the wetting of water by the oil TMPTMA. Interfacial tensions of the air/oil interface, γ_{ao} = 32.86 mN/m; of the oil/water interface, γ_{wo} = 18.99 mN/m; of the air/water interface (saturated with the oil), γ_{aw} = 51.74 mN/m. γ_{ao} and γ_{wo} were measured by axisymmetric drop shape analysis; γ_{aw} was measured with a ring tensiometer. The contact angles of the particles at the air/oil/particle and water/oil/particle interfaces are (a) $\Theta_{aop} = 6.7°$, $\Theta_{wop} = 114.7°$; (b) $\Theta_{aop} = 22.5°$, $\Theta_{wop} = 79.7°$; (c) $\Theta_{aop} = 36.6°$, $\Theta_{wop} = 53.2°$; (d) $\Theta_{aop} = 56.4°$, $\Theta_{wop} = 42.4°$. The structure of TMPTMA is shown in the inset.

Mixtures of TMPTMA (3.5 wt %), the photoinitiator benzoinisobutyl ether (0.175 wt %), and particles (0.5 wt %) in chloroform/ethanol (4:1 by weight) were applied to a water surface (927 cm^2) of a filled Langmuir trough (Lauda). After evaporation of the solvent, the surface pressure/area isotherms were recorded (Figure 2). Isotherms of the mixed layers containing TMPTMA and particles a, b, and d show one step in which the surface pressure steeply raises upon compression. The isotherm of particle c, on the other hand, shows two steps. The steps in the isotherms b, d and the first step in the isotherm c all occur near the area estimated for a close packed monolayer of these particles (dashed vertical lines in Figure 2). The isotherm c shows a second step occurring close to the area expected for a double layer (dotted vertical line in Figure 2), while the step in isotherm a occurs at an area between the area expected for a monolayer and a double layer. Therefore, one can conclude that the first step of c and the steps of b and d indicate the compression and finally collapse of a monolayer of

10.1021/ja058293p CCC: $33.50

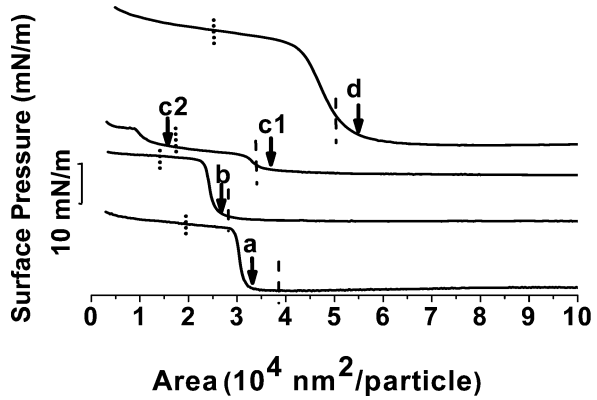

Figure 2. Surface pressure/area isotherms of the mixed layers containing particles and TMPTMA. Particle diameters a: $\Phi = 210$ nm $\pm$ 20 nm; b: $\Phi = 180$ nm $\pm$ 15 nm; c: $\Phi = 200$ nm $\pm$ 20 nm; d: $\Phi = 240$ nm $\pm$ 20 nm. The area calculation is based on a density of the particles of 1.9 g/cm^3. The vertical dashed and dotted lines indicate the area theoretically expected for a monolayer and for a double layer of particles. The arrows indicate the area per particle used for the experiments depicted in Figure 3.

particles, and the second step of c indicates that the monolayer of particle c undergoes a transition to a double layer which finally is compressed further into collapse. In the case of isotherm a, no clear interpretation based on the isotherm alone is possible. It is worth noting, however, that the area at which the step occurs moves closer to the expected area, the more hydrophobic the particles are (that is, in the order of a, b, c, d). It is therefore reasonable to assume that we lose a part of the particles into the water phase, and this loss is most pronounced in the case of the hydrophilic particles *a*.

To test the interpretation of the isotherms and the prediction of the theory, a second series of experiment was conducted. The mixed layers were compressed to the onset of the steps in the isotherms (see arrows labeled a, b, c1, c2, and d in Figure 2), solidified, and imaged with scanning electron microscopy.

These images (shown in Figure 3) confirm our expectations. For example, in the case of particles a and b, we theoretically expect and experimentally observe the formation of a monolayer of particles at the oil/water interface and no particles at the oil/air interface. In the case of particle d, we expect and observe a monolayer of particles adhering to the oil/air interface only (compare Figures 1 and 3). In the case of particle c, we expect a monolayer as in a and b; however, the position of particle c in the theoretical diagram is already close to the stability region of a double layer with particles adhering to the both interfaces. Thus, it is plausible that upon compression the monolayer undergoes a transition into the double layer shown in Figure 3c2. The structure of the monolayer at lower surface pressure, however, seems to deviate from our expectation (see c1 in Figure 3). While the scenario used in the theory assumes a monolayer of particles that is evenly covered by a layer of oil, we observe at most places of the sample a monolayer in which the particles are embedded in a thin layer of oil and protrude out of this layer at both interfaces (see Figure 3c1, left panel). At other places, the excess of the oil seems to form thicker lenses, the particles predominantly adhering to the upper surface of these lenses (see in Figure 3c1, right panel).

In conclusion, the investigations shown here demonstrate that the theoretical predictions agree at large with the experimental results. We observe all scenarios of wetting layers taken into account in the theoretical description. The position of the particles (on

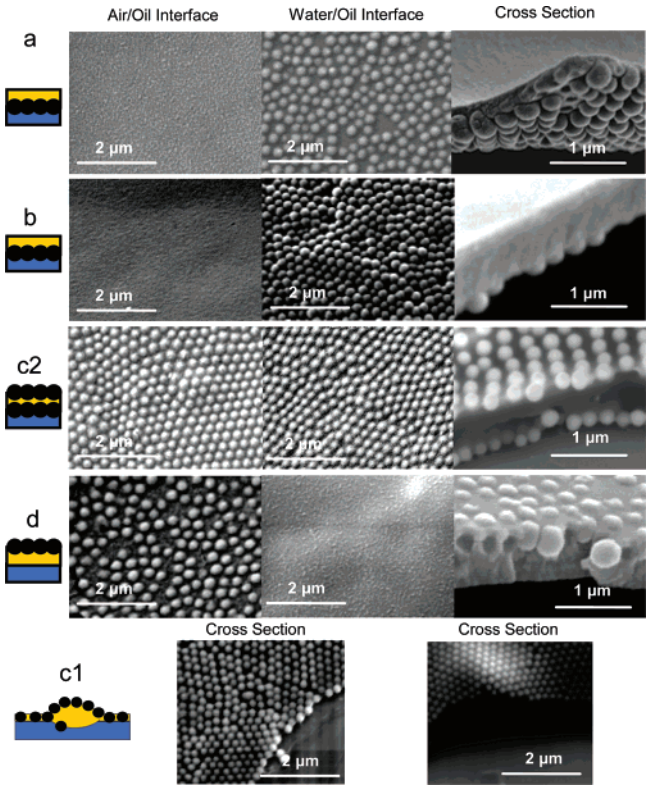

Figure 3. SEM images (by a Philips SEM 515 and a Nova NanoSEM 200) of the mixed layers of TMPTMA and particles formed on a water surface at the surface pressure indicated by the arrows in Figure 2. The mixed layers were solidified by photopolymerization and transferred to solid substrates by horizontal transfer.

bottom, top, or both interfaces of the wetting layer) can be influenced in agreement with the theory by choosing appropriate contact angles. In the fine print, we observe deviations: first, if the particles have similar affinities to both interfaces, the morphology of the layer is more complicated than expected; second, the experimentally observed morphology depends in addition on the surface pressure. It might therefore be necessary to extend the simple theoretical picture to take these observations into account.

Acknowledgment. We thank M. Hietschold, F. Müller, and S. Schulze for guidance in the operation of the SEM, and the Deutsche Forschungsgemeinschaft for support in initial stages of the work within the Research Training Group 328 of the University of Ulm.

References

(1) Xu, H.; Goedel, W. A. *Langmuir* **2003**, *19*, 4950−4952.
(2) Xu, H.; Goedel, W. A. *Angew. Chem., Int. Ed.* **2003**, *42*, 4694−4696.
(3) Xu, H.; Yan, F.; Tierno, P.; Marczewski, D.; Goedel, W. A. *J. Phys.: Condens. Matter* **2005**, *17*, S465−S476.
(4) Yan, F.; Goedel, W. A. *Chem. Mater.* **2004**, *16*, 1622−1626.
(5) Yan, F.; Goedel, W. A. *Adv. Mater.* **2004**, *16*, 911−915.
(6) Yan, F.; Goedel, W. A. *Nano Lett.* **2004**, *4*, 1193−1196.
(7) Marczewski, D.; Goedel, W. A. *Nano Lett.* **2005**, *5*, 295−299.
(8) Goedel, W. A *Europhys. Lett.* **2003**, *62*, 607−613.
(9) Clint, J. H.; Taylor, S. E. *Colloids and Surfaces* **1992**, *65*, 61−67.
(10) Binks, B. P.; Lumsdon, S. O. *Langmuir* **2000**, *16*, 8622−8631.
(11) Ding, A.; Binks, B. P.; Goedel, W. A. *Langmuir* **2005**, *21*, 1371−1376.
(12) Stöber, W.; Fink, A. Bohn, E. *J. Colloid Interface Sci.* **1968**, *26*, 62−69.
(13) Philipse, A. P.; Vrij, A. *J. Colloid Interface Sci.* **1989**, *128*, 121−136.
(14) Jesionowski, T.; Krysztafkiewicz, A. *Appl. Surf. Sci* **2001**, *172*, 18−32.

JA058293P